Computers and Electronics in Agriculture 178 (2020) 105756

Contents lists available at ScienceDirect

Computers and Electronics in Agriculture

journal homepage: www.elsevier.com/locate/compag

Modeling climate change impact on streamflow as affected by snowmelt in Nicolet River Watershed, Quebec

Qianjing Jiang[a], Zhiming Qi[a,*], Fei Tang[a], Lulin Xue[b], Melissa Bukovsky[b]

[a] Department of Bioresource Engineering, McGill University, Sainte-Anne-de-Bellevue, QC H9X 3V9, Canada
[b] National Center for Atmospheric Research, Boulder, CO 80307, USA

ARTICLE INFO

Keywords:
Climate change
Snowmelt
Streamflow
ArcSWAT
Peak flows

ABSTRACT

Frequent spring flooding in Southern Quebec's Nicolet River watershed has a history of causing severe damage, which is likely to worsen as climate change progresses. Employing the ArcSWAT model, an attempt was made to assess the potential impacts of climate change on the Nicolet River watershed's seasonal and annual streamflow, particularly that portion affected by snowmelt. Calibrated and validated against observed streamflow data for the periods of 1986–1990 and 1991–2000, respectively, the model reliably predicted daily streamflow (e.g., percent bias within ± 15%, Nash-Sutcliffe model efficiency > 0.50, and the ratio of root mean square error to the standard deviation ≤0.70). In an effort to investigate the impacts of climate change on streamflow, future climate datasets were generated for 2053–2067 by implementing the eleven sets of existing Regional Climate Model (RCM) simulations produced for the North American Regional Climate Change Assessment Program (NARCCAP) in the ArcSWAT model. The ArcSWAT model's hydrological responses were closely tied to changes of climate variables: a strong correlation existed between simulated runoff and precipitation, and between temperature and predicted evapotranspiration, snowfall, and winter snowmelt. Projected future climate data showed increases in both average temperature (+2.5 °C) and precipitation (+21%). Significant greater total precipitation was forecasted for the winter season, while total snowfall was projected to decrease by 6%. However, the snowmelt showed an increasing trend for the late winter and earlier spring period. Streamflow was expected to increase annually and in most seasons except spring. Annual peak flows volumes would increase by 13% in the future and the occurrence of peak flows would shift to the winter (*vs.* the spring), indicating a greater risk of winter flooding in the future. The individual impact of temperature and precipitation on peak flows showed that increases in peak flows were mainly tied to increased precipitation, while the shift in their timing was mostly tied to warming temperatures.

1. Introduction

It is widely acknowledged that the earth is warming due to increasing greenhouse gas emissions generated by anthropogenic activities (López-Ballesteros et al., 2020). Over the period of 1901–2012, the mean global temperature has risen by 0.89 °C (IPCC, 2013), and the warming is expected to continue (Zhang et al., 2019). In a recent governmental report released by Environment and Climate Change Canada, the mean annual temperature in Canada is expected to increase by 2.0–6.0 °C by 2100 (ECCC, 2019). With warmer temperatures, and the atmosphere's resulting greater capacity to hold water vapor, precipitation regimes will be altered (Rouhani and Leconte, 2018), and, accordingly the watersheds' hydrologic cycle. For snowmelt-dominated regions, changes in precipitation will affect snow accumulation and thereby streamflow, while changes in temperature will most likely influence the timing of snowmelt (Barnett et al., 2005). According to the Emergency Preparedness Canada (EPC) electronic disaster database, over 65% of the nation's flood disasters were attributed to snowmelt runoff, storm water, and storm rainfall runoff (Brooks et al., 2001). In the mountainous areas of the western United States, over 70% of runoff have been attributed to snowmelt (Li et al., 2017). Under a changing climate, higher latitude areas are more likely to experience increasingly extreme spring floods (Rouhani and Leconte, 2018). An analysis of Canadian hydrologic trends over the last 30 years has shown an increase in winter streamflow, a decrease in summer streamflow, along with earlier peak flows (Whitfield and Cannon, 2000; Zhang et al., 2000; St. Jacques and Sauchyn, 2009). A global analysis of climate change impacts on river flow regimes in a number of countries,

* Corresponding author.
E-mail address: zhiming.qi@mcgill.ca (Z. Qi).

https://doi.org/10.1016/j.compag.2020.105756
Received 3 June 2020; Received in revised form 23 August 2020; Accepted 28 August 2020

including Canada, predicted a significant increase in the magnitude of peak flows, but with their occurrence shifted at least one month earlier (Arnell and Gosling, 2013).

In Quebec, high flow events and spring floods are primarily the result of snowmelt, which accounts for up to 40% of annual streamflow (Coulibaly et al., 2000; Ferguson, 1999). Between 1900 and 1997, approximately 14% of the national flood disasters occurred in Quebec. The highly populated areas of southern Quebec have experienced a number of major flood events in the last few decades, and the recent one in 2017 has flooded thousands of houses and caused great damage to the riverside communities (Rouhani and Leconte, 2018). Under changing climate conditions, the occurrence of extreme spring floods in Quebec is predicted to increase, largely as the result of an earlier snowmelt (Beauchamp et al., 2015; Rouhani and Leconte, 2018). It is therefore essential to assess the potential impact of climate change on streamflow characteristics, especially peak flows, and thereby better monitor floods and offer watershed management adaptations to mitigate these disasters.

Hydrological models with snowmelt modules have been recently applied to simulate streamflow in snowmelt-dominated areas (Ficklin and Barnhart, 2014; Lachance-Cloutier et al., 2017; Tang et al., 2019). Accurate modeling and simulation of streamflow under snowmelt conditions typical of snow-dominated regionss are critical to capture watershed's physical and hydrological characteristics, and can provide guidance for local flood forecasting and control. In addition, the calibrated and validated models provide an option to forecast the long-term shifts in streamflow under various climate conditions. The ArcSWAT model is a semi-distributed hydrological model at a watershed-scale with different modules targeting various user demands (Arnold et al., 1998). Laying a solid foundation for further model application, the model provides accurate predictions of snowmelt-influenced streamflow at both daily and monthly time steps worldwide including West Seti River Basin (Bhatta et al., 2020), Himalayan River Basin (Bhatta et al., 2019), Heihe River Basin (Wu et al., 2015), Taleghan mountainous watershed (Noor et al., 2014), Outardes basin (Troin and Caya, 2014), Blue River watershed (Lemonds and McCray, 2007), Garonne watershed (Grusson et al., 2015), and Ontonagon River basin (Wu and Johnston, 2007).

Given its high accuracy and applicability towards long-term prediction of winter hydrological events in snow-dominated regions, several previous studies undertaken in southern Quebec have employed SWAT to investigate the hydrological response to climate change. These studies have suggested significant greater annual runoff, along with earlier snowmelt and discharge peaks (Gombault et al., 2015; Minville et al., 2008; Shrestha et al., 2012). Gombault et al. (2015) found that under future scenarios (2041–2070), spring floods would begin earlier, annual streamflow would increase by 9–19% and winter flow would increase by 2- to 3- fold as compared to the baseline period (1971–2000). While these studies were only concerned with the combined effects of temperature and precipitation on the peak flow of watersheds, the individual effects of temperature and precipitation changes on snowfall and snowmelt were not well addressed, an important omission since snowmelt is the major contributor to peak flows for the snow-dominated watersheds.

Located in the St Lawrence lowlands, the Nicolet River watershed has faced a growing risk of spring flooding in the recent years. In early April 2014, the watershed was added to a spring flood warning register, due to higher than normal water levels from spring thaw along and warming temperatures (CBC News, 2014). Road accesses to towns in this region were cut off because of high water levels in the spring of 2017. While no study of future streamflow in this watershed has been conducted, it is necessary to assess the impact of future climate change on the Nicolet River watershed hydrology, especially with respect to spring streamflow and snowmelt. Although Gombault et al. (2015) assessed the impact of climate change on the hydrology of the nearby Pike River watershed using a calibrated SWATqc model, they only applied four projected future climate datasets and there was a large variation among the four climate models in terms of spatial and seasonal changes. It is therefore necessary to apply multiple climate change models for the assessment of climate change impacts in this region.

The objectives of this study were to evaluate the ArcSWAT model's capacity to accurately simulate streamflow in a snow-dominated watershed, and subsequently, employing eleven projected climate scenarios, to quantify the potential impact of climate change on the Nicolet River watershed's hydrology as affected by snowmelt. This research focused on the hydrologic changes induced by climate change between the baseline period (1983–2000) and projected future climates (2050–2067), especially in the winter and spring seasons. Furthermore, both the combined and individual effects of temperature and precipitation change on future annual and seasonal streamflow as well as peak flow, as affected by snowmelt were assessed.

2. Materials and methods

2.1. Site description

The Nicolet River, as a southern tributary of the Saint Lawrence River, drains a watershed approximately 3380 km^2 into Lake Saint-Pierre. The research area intersected the downtown portions of the towns of Victoriaville and Warwick (Fig. 1). The stream flow data from hydrological station 02OD003 was downloaded from the Environment Canada's HYDAT database. Weather data, including precipitation and

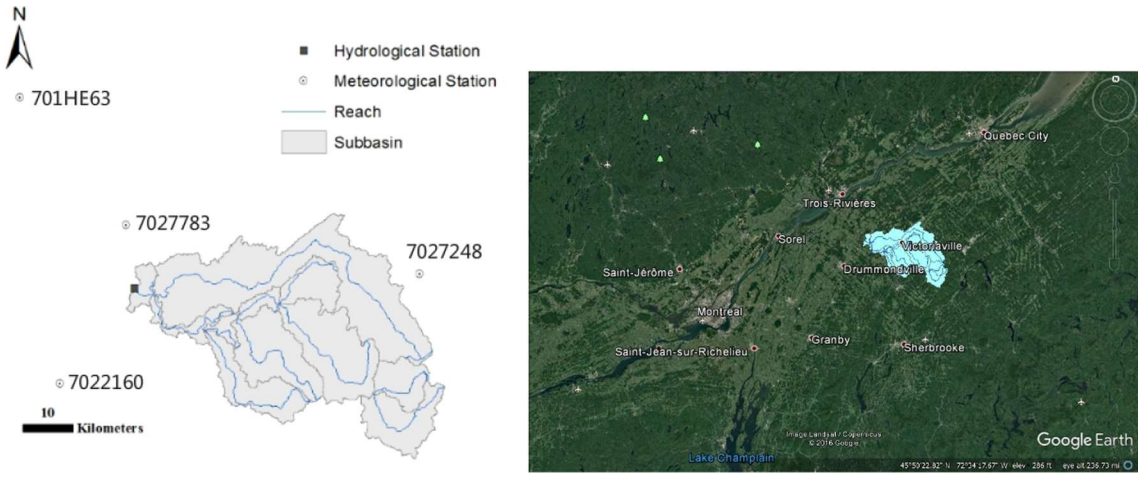

Fig. 1. Map of Nicolet watershed in southern Quebec, Canada.

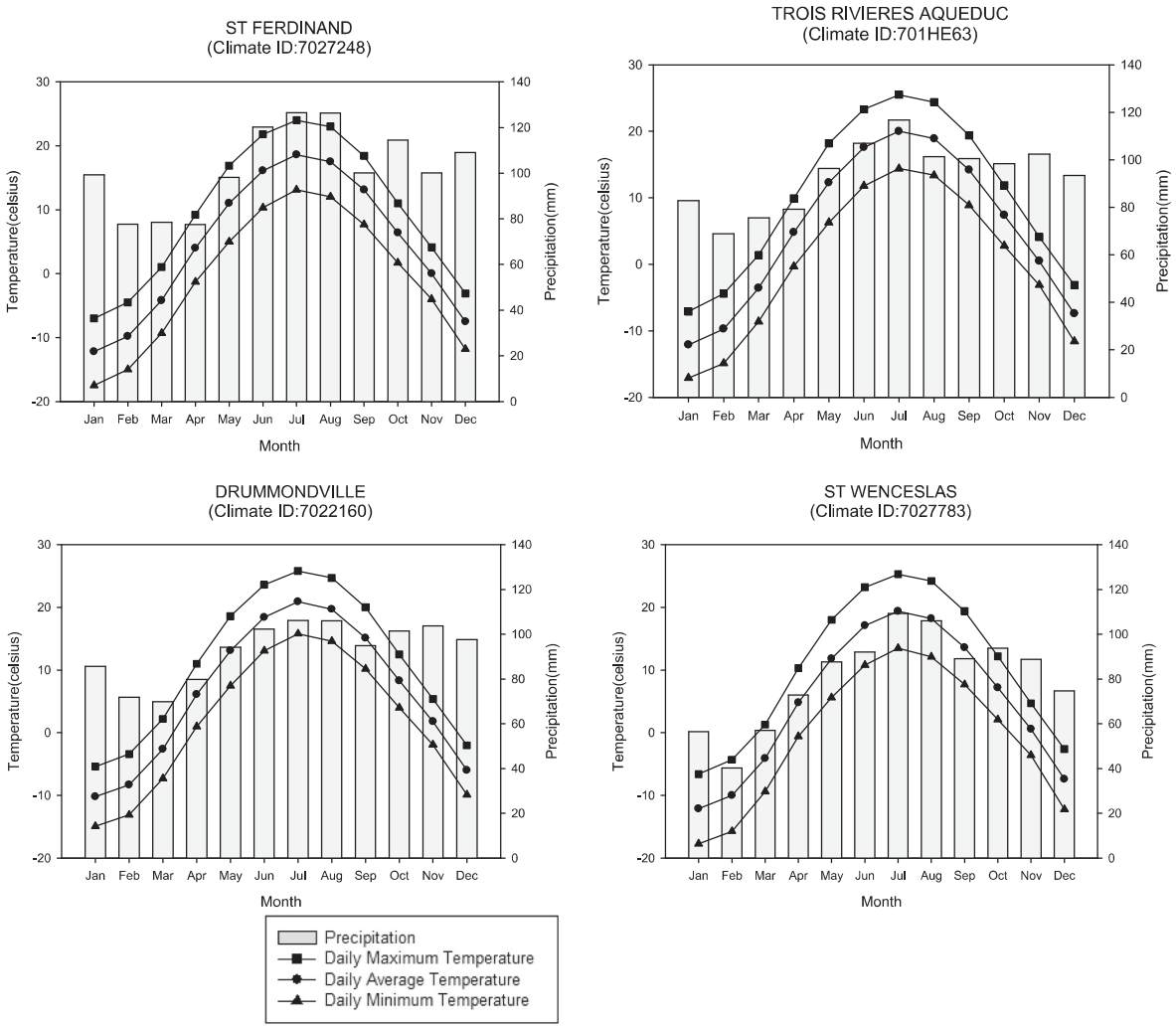

Fig. 2. Historical precipitation and temperature from 1981 to 2010 for the weather stations in the study area.

air temperature, were retrieved from four meteorological stations (Station ID: 701HE63; 7027783; 7022160; 7027248) within the watershed. The 30-year (1981–2010) Canadian Climate Normal Statistics for the four weather stations, were selected to provide the weather inputs (Fig. 2). Based on the weather station at St Ferdinand (Climate ID: 7027248), the average daily temperature of the study area was 4.4 °C and the mean annual precipitation of the study area was 1227.7 mm which consisted of 76.5% rainfall and 23.5% snowfall.

2.2. The overview of SWAT model

ArcSWAT, an ArcGIS extension and graphical user input interface for the Soil and Water Assessment Tool (SWAT) (Neitsch et al., 2011), was employed to simulate streamflow in this study due to its comprehensive capacity for hydrologic simulation. The SWAT is a semi-distributed hydrological model that simulates the hydrological processes in the watersheds, which was developed by the United States Department of Agriculture (USDA). Spatially-distributed data on topography, soils, land use, and meteorology were required for the model to simulate hydrological processes. The modeled watershed was divided into multiple sub-basins based on digital elevation data, then was further subdivided into hydrologic response units (HRUs) depending on soils, land use and slope features. The water balance in each HRU is subsequently computed to simulate the hydrologic processes (*e.g.*, precipitation, surface and subsurface flow, evapotranspiration, infiltration, groundwater, snow accumulation and snowmelt).

The snowmelt module in ArcSWAT utilizes the temperature index method to simulate the snowmelt processes. It assumes a linear relationship of the snowmelt and the difference between average maximum temperature and a threshold temperature. The snow accumulation is represented by the change of water content in snowpack. ArcSWAT classifies the precipitation as rainfall or snow based on mean daily air temperature, after which the liquid water equivalent of the snow precipitation is added to the snowpack if the air temperature is below the user-defined snowfall temperature. The timing and amount of snowmelt are determined by the combination of snowpack temperature, the melting rate and the areal coverage of snow. The snowmelt is included in the rainfall for calculating the runoff and infiltration (Neitsch et al., 2011).

2.3. Model setup

Datasets required by ArcSWAT model as input include a digital elevation model (DEM), soil type, land use, daily maximum and minimum air temperature, and precipitation.

2.3.1. Geographical data

A 90 m resolution DEM was acquired from the CGIAR Consortium for Spatial Information (CGIAR-CSI) originally provided by the NASA Shuttle Radar Topographic Mission (SRTM). DEM raster files were merged and projected to UTM Zone 19 N with datum WGS 1983. The watershed boundary and stream network were generated by the

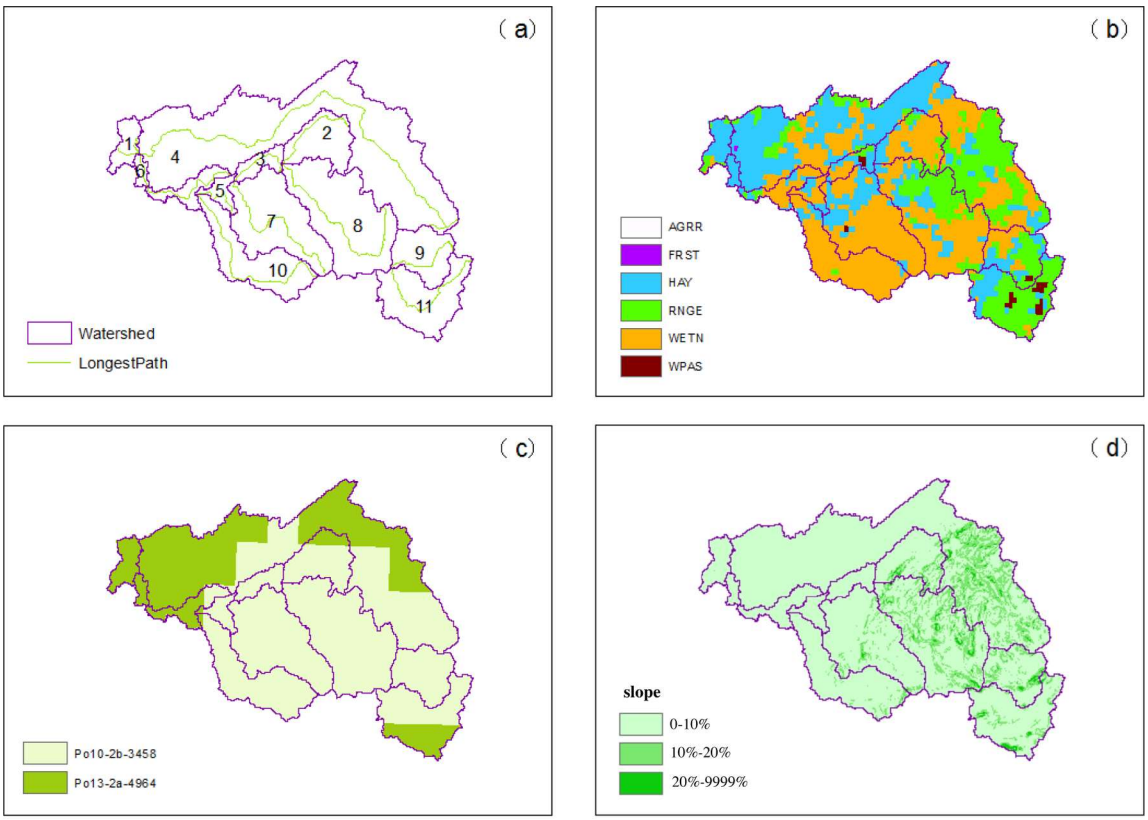

Fig. 3. Maps of delineated (a) watershed, (b) landuse, (c) soil type and (d) slope, Note: AGRR: Agriculture Land-Generic; HAY: Hay; FRST: Forest-Mixed; WETN: Wetland-Non-Forested; WPAS: winter tall fescue pasture; RNGE: Range-Grasees.

automatic watershed delineation tool in SWAT based on the DEM. Land use data was accessed from the WaterBase database, and a resampled version with a resolution of 800 m was applied in the study area. Detailed topical water maps for the watershed are shown in Fig. 3. Hay (HAY), Forest-Mixed (FRST), and Wetland-Non-Forested (WETN) were identified as the dominant land uses (Fig. 3b). The soil information was drawn from the FAO-UNESCO soil map shown in the Supplemental Material. In the current study area, two types of soil (Po13-2a-4964; Po10-2b-3458) were represented as the primary soil types (Fig. 3c), both of which were loams and belonged to class C (see Supplemental Material Table S1), indicating slow infiltration rates, low rates of water transmission and high runoff potential.

2.3.2. Meteorological and hydrological data

The historical meteorological data from 1983 to 2000 was obtained from four weather stations in the catchment (ID: 701HE63; 7027783; 7022160; 7027248) from the website of Environment Canada. The data include daily maximum and minimum temperature, as well as precipitation. The coordinates of each weather station are shown in Table 1.

Drawing on Environment Canada's HYDAT database, historical stream flow data was obtained from a hydrologic station (ID: 02OD003, 46°03′23″ N, 72°18′23″ W) situated 5.8 km from the mouth of the Bulstrode River, a northern branch of Nicolet River. The seasonal streamflow followed a pattern where spring flow, affected by snowmelt, contributed most of the runoff volume. The discharge declined gradually from late autumn to winter, and then reached to minimum value in early spring of the next year.

Table 1
The geographical information of weather stations.

Station Name	Station ID	Longtitude	Latitude
TROIS RIVIERES AQUEDUC	701HE63	72°62′ W	46°38′ N
ST WENCESLAS	7,027,783	72°33′ W	46°17′ N
DRUMMONDVILLE	7,022,160	72°48′ W	45°88′ N
ST FERDINAND	7,027,248	71°58′ W	46°10′ N

2.4. Model calibration and validation

The whole period of 1983–2000 was divided into three sub-periods, which were used for model initialization and warm up (1983–1985), model calibration (1986–1990) and model validation (1991–2000). The simulated daily and monthly streamflow were compared with observed values for the evaluation of model performance based on statistical analysis. To understand the hydrologic components of a watershed, it is necessary to analyze the water yield, which is defined as the aggregate sum of water leaving the HRU and entering the principle channel (Arnold et al., 2012a,b). SWAT Check was executed for default output after each run to examine the availability of water in each hydrological component, including the amount of precipitation, evapotranspiration, groundwater, surface runoff, soil water content and water yield. Water balance equations were employed to assess the rationality of model output and provide a guide for calibrating the model. The total water yield and water balance error are calculated as:

$$WYLD = Q_{surf} + Q_{lat} + Q_{gw} - T_{loss} - POND \quad (1)$$

$$Water\ \ balance\ \ error = P - (WYLD + ET + \Delta S + DS) \quad (2)$$

where WYLD is the total water yield (mm), Q_{surf} is the surface runoff contribution to streamflow (mm), Q_{lat} is the lateral flow contribution to streamflow (mm), Q_{gw} is groundwater contribution to streamflow (mm), POND is the pond abstractions (mm), T_{loss} is the transmission loss from tributary channels (mm), P is the total precipitation (mm), ET is the evapotranspiration (mm), ΔS is the change in soil water storage (mm), and DS is the deep seepage (mm).

Table 2
Results of sensitivity analysis for water yield (WY), surface flow (SF) and subsurface flow (SSF).

Parameter	Sensitivity Rank			Range		WY (mm)		SF (mm)		SSF (mm)	
	WY	SF	SSF	Min	Max	Min	Max	Min	Max	Min	Max
CN2	–	1	4	74	86	499.76	500.81	154.12	284.09	204.85	326.72
GW_REVAP	3	–	3	0.02	0.2	377.02	499.76	212.07	212.07	149.48	272.22
ESCO	1	3	5	0.01	1	391.43	561.89	197.62	213.49	183.07	287.15
SLSOIL	4	2	1	0	150	371.55	425.45	167.87	212.32	0	272.22
SOL_AWC	2	–	2	0	1	354.39	489.79	208.46	214.49	213.29	337.71

Note: CN2 is initial SCS runoff curve number for moisture condition II, GW_REVAP is groundwater "revap" coefficient, ESCO is soil evaporation compensation factor, SLSOIL is lope length for lateral subsurface flow, SOL_AWC is available soil water content, Min is minimal, and Max is maximal.

2.4.1. Sensitivity analysis

Before model calibration, a local sensitivity analysis approach allowing parameters to change gradually from maximum to minimum values one at a time while all the other parameters unchanged, as suggested by the guidelines of Arnold et al. (2012b) and Marin et al. (2020), was employed to determine the key parameters and their ranges of sensitivity (Arnold et al., 2012a). Sensitivities were defined by the percentage change in surface and subsurface runoff or water yield, with respect to changes in the parameters. For streamflow and snowmelt, fifteen parameters that are frequently reported as being sensitive were selected for the sensitivity analysis. The parameters were ranked by the level of their influence on the model output based on the sensitivity test, and the five most sensitive parameters from current study are shown in Table 2. The soil evaporation compensation factor (ESCO) was the most sensitive parameter for water yield, which directly controlled the amount of available water in soil layers for soil evaporation. The runoff curve number (CN2) was the most sensitive parameter for surface runoff, however, changes in CN2 did not evidently affect the result of water yield due to its negative impact on subsurface flow and groundwater, which made it a key parameter to partition precipitation into infiltration and runoff. The subsurface flow was found to be notably influenced by the slope length of soil (SLSOIL). The groundwater "revap" coefficient (GW_REVAP) controlled the water movement from the shallow aquifer to the root zone, while the available water capacity of the soil layer (SOL_AWC) played a crucial role in determining both subsurface flow and water yield.

2.4.2. Model calibration and validation

The calibrated values for the 15 relevant parameters are shown in Table 3. The value of CN2 was increased by 11% in order to increase runoff and reduce infiltration. The ESCO was adjusted from a default value of 0.95–0.65 to allow more water extraction for evaporation from deep soil layers, thus increasing the evapotranspiration in summer. The groundwater "revap" coefficient (GW_REVAP) was increased from 0.02 to 0.05, to transfer more water from shallow aquifer to the root zone. Although available soil water content (SOL_AWC) and slope length for lateral subsurface flow (SLSOIL) were sensitive parameters for streamflow, the two values were kept at default values as changes in those two values did not achieve a better simulation in streamflow (Table 3). In addition to the five most sensitive parameters, several more parameters as listed below were adjusted to optimize predicted results. Given the soil's slow rate of water transmission and infiltration in the study region (Class C, Table S1), the GW_DELAY, which denotes the time that water infiltrates through the soil layers into the shallow aquifer, was reset from the default of 31 days to 80 days. The value of ALPHA_BF was increased from a default value of 0.048 to 0.5 to decrease summer baseflow. While the sensitive parameters had a primary impact on the amount of the water available for each component, the timing of the streamflow peaks for the tributary channels was controlled by average slope length (SLSUBBSN), average slope steepness (SLOPE), and Manning's "*n*" value (CH_N1). Accordingly, the SLSUBBSN was increased by 10%, while the SLOPE was decreased by 20% to shorten the time of concentration. As suggested by Arnold et al. (2012b), for the land covered by moderate vegetation, CH_N1 was adjusted from 0.014 to 0.05.

Based on the sensitivity analysis undertaken in the current study, four out of seven snowmelt-related parameters were among the most sensitive parameters controlling the snowmelt process: SFTMP, SMTMP, SMFMX and SMFMN. Defined as the snowfall temperature, SFTMP was decreased from 1 °C to −1 °C to increase snowfall and postpone snowmelt. Snowmelt base temperature above which snowpack melts, SMTMP, was increased from 0.5 °C to 3.5 °C to better simulate stream flow, which, in turn, decreased the volume of peak flows in winter, and divided a major peak into several sub-peaks. The impact of snowpack density on snowmelt was represented by SMFMX and SMFMN, which were both increased from their default values of 4.5 °C to 5 °C and 5.5 °C, respectively (Lévesque et al., 2008). In addition, SNOCOVMX and SNO50COV, suggested as top parameters affecting the

Table 3
Calibrated parameters for the SWAT model.

Parameters	Definition	Unit	Default value	Optimal value
CN2	Initial Soil Conservation Service (SCS) runoff curve number for moisture condition	–	–	+11%
GW_REVAP	Groundwater "revap" coefficient for water movement from shallow aquifer to root zone.	–	0.02	0.05
ALPHA_BF	Baseflow alpha factor	days	0.048	0.5
GW_DELAY	Groundwater delay time	days	31	80
ESCO	Soil evaporation compensation factor	–	0.95	0.65
CH_N1	Manning's "n" value for the tributary channels	–	0.014	0.05
SURLAG	Surface runoff lag coefficient	–	2	1.3
SLOPE	Average slope steepness	m/m	–	−20%
SLSUBBSN	Average slope length	m	–	10%
SFTMP	Snowfall temperature		1	−1
SMTMP	Snow melt base temperature		0.5	3.5
SMFMX	Melt factor for snow on June 21		4.5	5
SMFMN	Melt factor for snow on December 21		4.5	5.5
SNOCOVMX	Minimum snow water content that corresponds to 100% snow cover	mm	1	50
SNO50COV	Fraction of snow volume represented by SNOCOVMX that corresponds to 50% snow cover	–	0.5	0.2

unevenly distributed areal snow cover by Yang et al. (2014) , were adjusted and shown in Table 3.

2.5. Assessment of model performance

According to the guidelines by Moriasi et al. (2007), the Nash-Sutcliffe efficiency (NSE, Nash and Sutcliffe, 1970), root mean square error (RMSE)-observations standard deviation ratio (RSR), and percent bias (PBIAS) were adopted in this study to evaluate the performance of ArcSWAT in modeling the streamflow in the Nicolet River watershed. An NSE value of 1 indicates a perfect match of model simulation and observation, while a value less than 0 indicates that the observed mean is a more accurate predictor than the simulated result. The model performance is considered as "satisfactory" when NSE is greater than 0.5, "good" when $0.65 \leq NSE \leq 0.75$, and "very good" when $NSE \geq 0.75$ (Moriasi et al., 2007, 2015). The RMSE-observations standard deviation ratio (RSR) was selected as it represents both an error index and a normalization factor applicable to various constituents. The optimal RSR value of 0 indicates zero RMSE, and the simulation is considered acceptable when RSR is less than 0.7 (Singh et al., 2005). PBIAS measures the difference between simulated and observed values. The optimal value of PBIAS is 0, while positive and negative values indicate underestimation and overestimated of bias, respectively. The model performance is judged as satisfactory when PBIAS is within ± 15% (Moriasi et al., 2007, 2015). These statistics are calculated as:

$$NSE = 1 - \left[\frac{\sum_{i=1}^{n} (Y_i^{obs} - Y_i^{sim})^2}{\sum_{i=1}^{n} (Y_i^{obs} - Y_i^{mean})^2} \right] \quad (3)$$

$$RSR = \frac{\sqrt{\sum_{i=1}^{n} (Y_i^{obs} - Y_i^{sim})^2}}{\sqrt{\sum_{i=1}^{n} (Y_i^{obs} - Y_i^{mean})^2}} \quad (4)$$

$$PBIAS = 100 \times \frac{\sum_{i=1}^{n} (Y_i^{obs} - Y_i^{sim})}{\sum_{i=1}^{n} Y_i^{obs}} \quad (5)$$

2.6. Climate scenarios

The future climate datasets were generated by the North American Regional Climate Change Assessment Program (NARCCAP), an international program providing high solution climate scenarios for North America (Mearns et al., 2007, 2009). Regional climate models (RCMs) were embedded into General Circulation Model (GCMs) to obtain regional climate data at a spatial resolution of 50 km. Eleven sets of climate scenarios obtained through different RCMs-GCMs pairings served as future meteorological data. Current climate projections (1971–1998) and future climate projections (2038–2068) were generated for each climate scenarios. The historical observed weather data from 1983 to 2000 from four meteorological stations (Climate ID: 701HE63; 7027783; 7022160; 7027248) were averaged and drawn upon in baseline scenarios.

The projected future climate data were not always representative of the current climate conditions as some unreasonable low (below 0 °C) summer temperatures were present. Therefore, the change factor (CF) method was employed to correct the bias between modeled and observed climate data (Chen et al., 2011; Minville et al., 2008). To obtain the differences between projected future and current climate data, we generated historical (1983–2000) and future (2050–2067) daily weather data for four weather stations using all eleven climate models. Then the monthly differences between historical and future data were calculated, and subsequently changes in temperature (°C) and precipitation (%) were added to the baseline scenario weather data, and finally future scenarios were generated (See equations in Supplemental Material).

2.7. Future climate data

The mean annual temperature under baseline (1983–2000) conditions was 4.2 °C, and increased by 2.5 °C in future weather projections (2050–2067) (Table S2, in Supplemental material). All scenarios showed increases in future annual mean temperature for the Nicolet River watershed, ranging from 2.0 °C to 3.1 °C. The mean seasonal temperature changes were +2.1 °C, +2.2 °C, +2.5 °C and +3.2 °C for spring (March 21-June 20), summer (June 21-September 20), autumn (September 21-December 20), and winter (December 21-March 20), respectively. The projected changes in future (+67 years) air temperatures in Quebec were greater than those observed changes in historical data (Yagouti et al., 2008) where annual mean temperature increased significantly from 0.6° to 1.8 °C over the period of 1960–2005, with the warming trend being more pronounced in winter than summer. Our projected future climate was comparable with that generated by DesJarlais et al. (2010), who predicted increases in future temperature of 2.5 °C to 3.8 °C in winter and 1.9 °C to 3.0 °C in the summer by 2050. The large increases in winter and spring temperatures may result in a reduction of snow accumulation and an increase in snowmelt, thus affecting streamflow.

Mean annual precipitation increased from 1230 mm under the baseline, to 1487 ± 88.5 mm (+21%) in the future averaged across all scenarios. Seasonally, the precipitation increased by 52 mm (+20%), 59 mm (+18%), 60 mm (21%) and 84 mm (+27%) for spring, summer, autumn, and winter, respectively. Among different scenarios, percent change in precipitation varied from 6% to 35% for spring, 8% to 42% for summer, 3% to 42% for autumn and 16% to 52% for winter. This range of variation in climate change parameters could raise the complexity of water flow dynamics, which are interactively affected by the precipitation, temperature and snowmelt. In addition, the large variability between different climate models may result in great variance in hydrologic responses.

3. Results and discussion

3.1. Model calibration and validation

The simulated streamflow closely matched the observed streamflow in both calibration and validation periods (Fig. 4). After model calibration, the model showed satisfactory model performance for simulating both the daily flow (NSE = 0.55, RSR = 0.67, and PBIAS = 9%) and monthly streamflow (NSE = 0.75, RSR = 0.50 and PBIAS = 9%) with an overall water balance error of 5% (Table 4). Validated over the period of 1996–2000 on both daily and monthly time steps, the ArcSWAT model showed adequate model performance in simulating both monthly (NSE = 0.51, RSR = 0.69, and PBIAS = 2%) and daily (NSE = 0.84, RSR = 0.49 and PBIAS = 2%) streamflow, including spring streamflow predominantly attributed to snowmelt. Overall, the model accurately simulated the timing of peak flows, although the volume of peak flow was slightly (2%) underestimated.

Our calibration and validation accuracy results were better than those of Gombault et al. (2015) who achieved acceptable model performance of SWATqc for predicting monthly streamflow (NSE = 0.55) in the validation phase, but an unacceptable performance in the calibration phase (NSE < 0.50) for Quebec's Pike River watershed. The authors attributed the poor accuracy to SWAT's inability to effectively capture high-intensity, short-duration rainfall events at a daily time step. In the present case, the statistics for both calibration and validation phases demonstrated that the SWAT model was reliable in

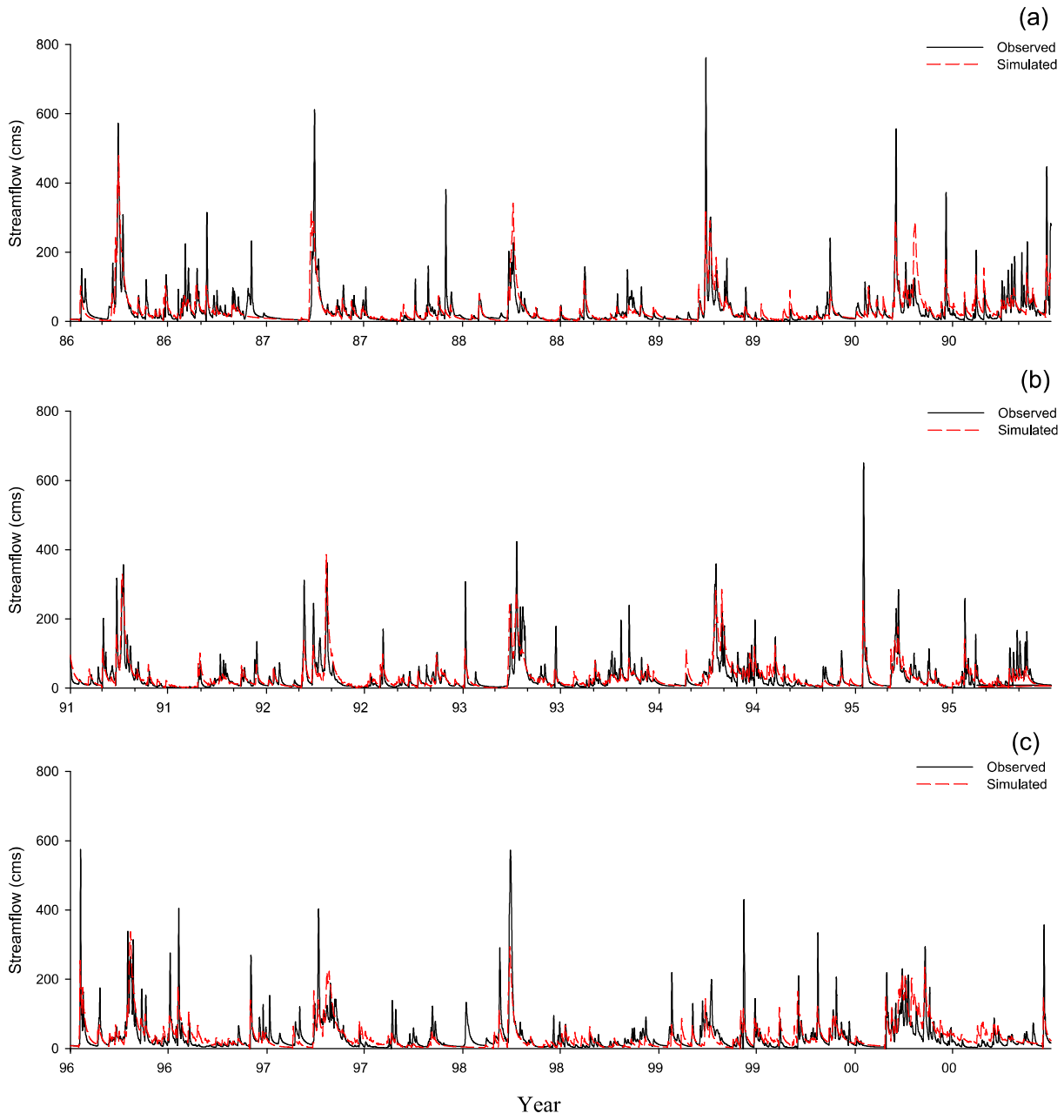

Fig. 4. Comparison of simulated and observed streamflow in the (a) calibration from 1986 to 1990 and (b and c) validation from 1991 to 2000.

Table 4
Statistics of calibrated and validated results for monthly and daily streamflow.

Period	Time Step	NSE	RSR	PBIAS
Calibration (1986–1990)	Daily	0.55	0.67	9%
	Monthly	0.75	0.50	9%
Validation (1991–2000)	Daily	0.51	0.69	2%
	Monthly	0.77	0.48	2%

representing the physical and hydrological characteristics in the study area.

3.2. Hydrologic responses to climate change

3.2.1. The volume of annual and seasonal streamflow

Comparison of the annual and seasonal streamflow between baseline (1983–2000) and future scenarios (2050–2067), showed that the historical mean annual streamflow rate of 31.9 $m^3 s^{-1}$, was predicted to increase by 25% to 39.3 ± 4.6 $m^3 s^{-1}$ in the future (Table 5). All future scenarios demonstrated increases in predicted future annual streamflow; however, the greatest variations in annual streamflow simulation occurred between different projected climatic datasets, with the largest increase in mean annual streamflow produced by ECP2_HadCM3 (47.2%) and the smallest by WRFG_CCSM (8%). Although reports have provided conflicting results regarding global streamflow rates trends, a consistent trend of increased observed streamflow has been found for cold high latitude regions (Sharma and Wasko, 2019). Our prediction of greater annual streamflow concurred with many studies undertaken in snow-dominant regions (Shrestha et al., 2017; Zhao et al., 2019). The changes in annual streamflow volume were mainly resulted from altered precipitation rather than shifts in temperature, indicating that precipitation depth was the dominant factor for annual streamflow volume (Hammond et al., 2018; Tang et al., 2019).

For the seasonal discharge, simulations under all climate scenarios

Table 5
Seasonal and annual streamflow under baseline (1983–2000) and future climate scenarios (2050–2067).

Climate Scenarios	Streamflow (m^3 s^{-1})				
	Spring	Summer	Autumn	Winter	Annual
Baseline	59.2	24.1	20.8	23.5	31.9
CRCM_CCSM	56.8	27.5	23.5	37.1	36.2
CRCM_CGCM3	61.6	27.5	23.7	42.4	38.8
ECP2_GFDL	60.6	33.6	25.4	51.8	42.9
ECP2_HadCM3	55.7	44.3	38.3	49.4	46.9
HRM3_HadCM3	56.2	28.8	30.6	42.3	39.5
MM5I_CCSM	60.8	41.6	37.3	44.9	46.1
MM5I_HadCM3	49.0	29.3	25.0	39.9	35.8
RCM3_CGCM3	57.7	33.3	27.8	40.1	39.7
RCM3_GFDL	61.9	28.0	23.5	35.8	37.3
WRFG_CCSM	51.2	31.1	19.7	36.9	34.7
WRFG_CGCM3	67.1	31.4	29.8	37.6	41.5
Future average	58.1	32.4	27.7	41.7	39.9
Change	−2%	+34%	+33%	+77%	+25%

suggested increased amounts of total streamflow in summer, autumn and winter. However, there was no consensus on spring stream flow among different climate scenarios. Whereas the CRCM_CCSM, ECP2_HadCM3, HRM3_HadCM3, MM5I_HadCM3, RCM3_CGCM3 and WRFG_CCSM scenarios suggested decreases, the remaining scenarios suggested increases in spring streamflow. Although precipitation was projected to increase by 20% (+52 mm) in future springs, averaged across all future climate scenarios spring streamflow decreased slightly to 1.1 m^3 s^{-1} (2%), compared with the baseline period. Our predicted change in spring streamflow was on the order of that reported by Gombault et al. (2015), implying a slight decrease of streamflow from January to March. The decrease in spring streamflow could be mainly attributed to an earlier snowmelt, which was historically concentrated in April but moved to between January and March in the future scenario (Fig. 5b). Accordingly, the greatest increase of streamflow was forecasted for the winter, with an average increase of 77% compared to the baseline, while a more moderate increase as forecasted to occur in the summer and fall (slightly over 30%), because increases in evapotranspiration partially offset the impact of increasing precipitation on streamflow (Table 5).

3.2.2. Peak flows

The change in daily peak flow was analyzed based on the snow pattern (Fig. 5), magnitude of peak discharge (Fig. 6), and the timing of peak occurrences. The changes in the timing of peak flows were quantified as the frequency of peak flow occurrences in each month (Table 6). For the volume of peak flows, CRCM_CCSM, MM5I_HadCM3,

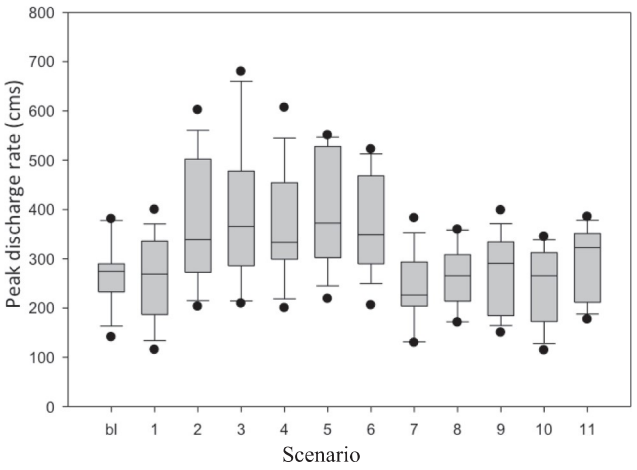

Fig. 6. Annual peak discharge rates for future scenarios (2050–2067) and baseline (1983–2000). Note of x-axis and y-axis legends: bl: baseline; 1:CRCM_CCSM; 2:CRCM_CGCM3; 3:ECP2_GFDL; 4:ECP2_HadCM3; 5:HRM3_HadCM3; 6:MM5I_CCSM; 7:MM5I_HadCM3; 8:RCM_CGCM3; 9:RCM3_GFDL; 10:WRFG_CCSM; 11:WRFG_CGCM3; cms: cubic meters per second.

RCM3_CGCM3 and WRFG_CCSM suggested slight decreases (median value) in annual peak flow volume, whereas the remaining scenarios showed increases (median value) ranging from 6% to 36%. However, there was no significant ($p > 0.05$) difference in the magnitude of peak flows between baseline and future scenarios. Burn and Elnur (2002) suggested that the magnitude of peak flows had not significantly changed since 1970 for more than 80% of the rivers in Canada. On average, the volume of annual peak flow increased by 13% compared to the baseline period (Fig. 6), whereas the total snowfall and snowmelt were predicted to decrease by 6.5% (Fig. 5a) and 4.4% (Fig. 5b), respectively. As a result, the proportion of snowmelt contributing to peak flow was projected to decrease as well. Therefore, the increases in the volume of peak flows in the future are more likely attributable to an increase in rainfall.

For the timing of peak discharge, all scenarios implied earlier occurrences of the peaks (Table 6). During the baseline period, the majority of peak flows occurred in March (27%) and April (40%), whereas, under future scenarios peak flows were re-distributed, with 51% in March and 13% in April. The number of peak flows events in March increased from 4 events under the baseline to 7.6 events in the future, while the number of peak flows in April decreased from 6 events under the baseline to 2 events in the future. Moreover, the number of peak flow events in the winter (January, February and March) increased

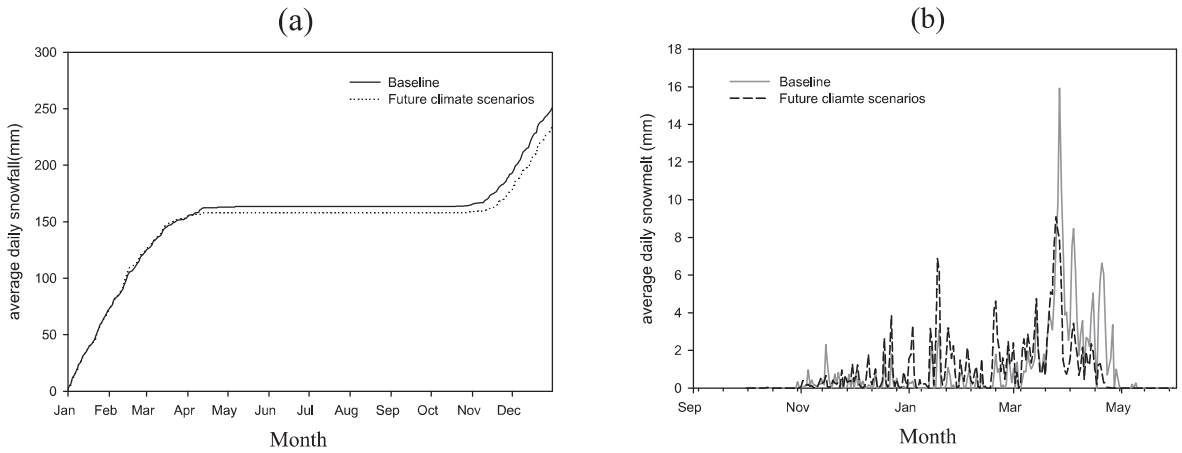

Fig. 5. Annual (a) accumulated snowfall and (b) snowmelt for the average of 11 future climate scenarios (2050–2067), and for baseline period 1983–2000.

Table 6
Number of the peak flow events in each month in baseline (1983–2000) and future scenarios (2050–2067). Months with no peak flows are not shown.

	Jan	Feb	Mar	Apr	May	Aug	Sep	Nov	Dec
Baseline	2	–	4	6	2	–	1	–	–
CRCM_CCSM	3	–	8	3	–	–	1	–	–
CRCM_CGCM3	2	1	8	2	–	–	–	–	2
ECP2_GFDL	5	1	3	4	–	–	–	–	2
ECP2_HadCM3	2	1	5	–	–	3	1	1	2
HRM3_HadCM3	2	3	7	2	–	–	1	–	–
MM5I_CCSM	3	–	6	2	–	3	–	–	1
MM5I_HadCM3	4	1	7	1	1	–	1	–	–
RCM3_CGCM3	2	–	9	2	–	–	1	–	1
RCM3_GFDL	2	–	10	2	–	–	1	–	–
WRFG_CCSM	3	1	10	1	–	–	–	–	–
WRFG_CGCM3	2	–	11	1	–	–	1	–	–
Future average	2.7	0.7	7.6	2.0	0.1	0.5	0.6	0.1	0.7
Change	+0.7	+0.7	+3.6	−4.0	−1.9	+0.5	−0.4	+0.1	+0.7

dramatically by 83% from 6 events under the baseline to 11 events in the future, while the occurrence in spring (April, May and June) decreased by 74% from 8 to 2.1. It should be noted that the possibility of flooding was predicted to be greater in January (2.7 events) than April (2 events). The redistribution of peak flows indicated a greater risk of winter flooding, and the spring flood tended to occur earlier in March instead of April as usual. The present study's prediction of earlier peak flow events was consistent with Cunderlik and Ouarda (2009), who analyzed historical streamflow data from 229 stations across Canada and suggested that significant earlier peak flows had been brought on by the occurrence of spring snowmelt in most of the regions of Southern Canada. Our results were also consistent with those of Aygün et al. (2019), who reviewed the impacts of global climate change on hydrology in cold regions and found a consistent trend of earlier occurrence of snowmelt floods and increased streamflow in winter over previous years.

3.2.3. *Individual impact of temperature and precipitation*

Using the calibrated and validated ArcSWAT model, the individual impact of changes in temperature and precipitation on peak flows was assessed by changing each variable at a time and keeping another at the same level as under the baseline. With the change in precipitation only, the predicted annual volume of future peak flows increased by 7% compared with the baseline (Fig. 7a). The future distribution of monthly peak flows followed a similar pattern to baseline, with most future peak flows (48%) occurring in April, compared to 40% under the baseline (Table 7). The average snowfall was predicted to increase

Table 7
Number of peak flow events in each month for baseline (1983–2000) and future (2050–2067) scenario with only precipitation change (Months with no peak flows are not shown).

Climate Scenarios	Jan	Mar	Apr	May	Jun	Aug	Sep	Dec
Baseline	2	4	6	2	–	–	1	–
CRCM_CCSM	1	5	7	2	–	–	–	–
CRCM_CGCM3	1	9	5	–	–	–	–	–
ECP2_GFDL	–	1	7	7	–	–	–	–
ECP2_HadCM3	1	2	9	2	–	–	1	–
HRM3_HadCM3	1	4	7	2	–	–	1	–
MM5I_CCSM	1	4	5	–	–	3	1	1
MM5I_HadCM3	1	4	8	2	–	–	–	–
RCM3_CGCM3	1	4	7	2	–	–	1	–
RCM3_GFDL	1	3	9	1	–	–	1	–
WRFG_CCSM	1	4	7	2	1	–	–	–
WRFG_CGCM3	1	3	8	2	–	–	1	–
Future average	0.9	3.9	7.2	2.0	0.1	0.3	0.5	0.1
Change	−1.1	−0.1	+1.2	0.0	+0.1	+0.3	−0.5	+0.1

significantly by 28% under the future scenarios, which means more snow was accumulated in the snowpack for later melt (Fig. 8a). As a result, the amount of snowmelt was forecasted to increase over the full snowmelt season (Fig. 9a), though a slight decrease in snowmelt peaks was found.

With the change in temperature only, the volume of peak flows was predicted to decrease by 5% compared with the baseline (Fig. 7b), and the timing of future peak flows' occurrence was evidently advanced

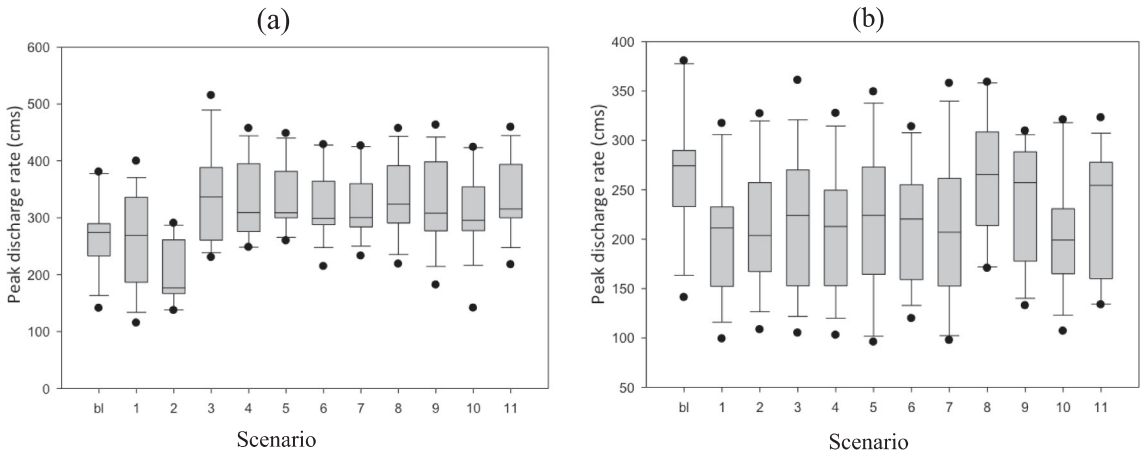

Fig. 7. Individual impact of changing (a) precipitation and (b) temperature on annual peak discharge rates in future climate scenarios (2050–2067) and baseline (1983–2000), Note of x-axis legends: bl: baseline; 1:CRCM_CCSM; 2:CRCM_CGCM3; 3:ECP2_GFDL; 4:ECP2_HadCM3; 5:HRM3_HadCM3; 6:MM5I_CCSM; 7:MM5I_HadCM3; 8:RCM_CGCM3; 9:RCM3_GFDL; 10:WRFG_CCSM; 11:WRFG_CGCM3.

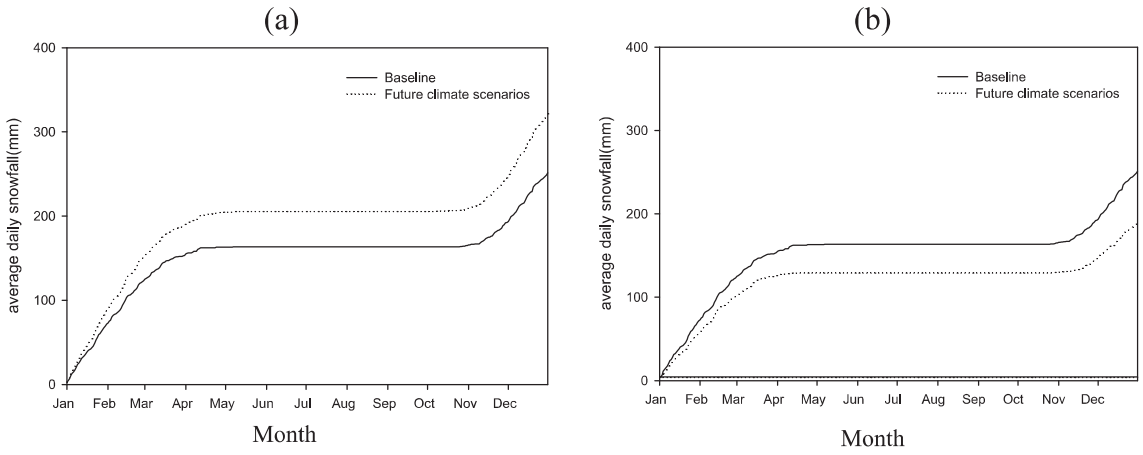

Fig. 8. Individual impact of changing (a) precipitation and (b) temperature on average daily snowfall in the average of 11 future climate scenarios (2050–2067) and baseline (1983–2000).

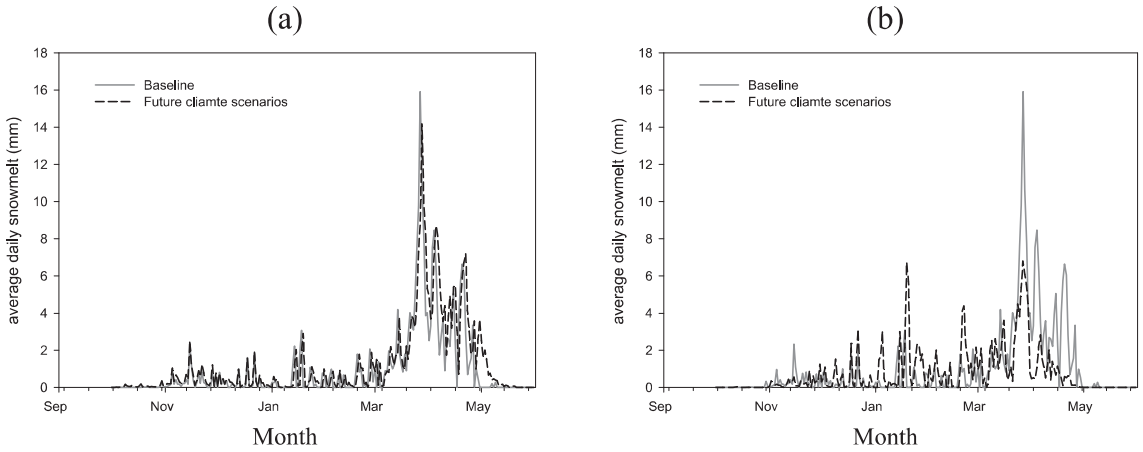

Fig. 9. Individual impact of changing (a) precipitation and (b) temperature on average daily snowmelt in the average of 11 future climate scenarios (2050–2067) and baseline (1983–2000).

Table 8
Number of peak flow events in each month for baseline (1983–2000) and future (2050–2067) scenario with only temperature change (Months with no peak flows are not shown).

Climate Scenarios	Jan	Feb	Mar	Apr	May	Aug	Sep	Dec
Baseline	2	–	4	6	2	–	1	–
CRCM_CCSM	4	–	8	2	–	–	1	–
CRCM_CGCM3	3	–	9	2	–	–	–	1
ECP2_GFDL	4	1	7	2	–	–	1	–
ECP2_HadCM3	5	1	6	2	–	–	–	1
HRM3_HadCM3	3	3	6	–	1	1	–	1
MM5I_CCSM	3	–	9	2	–	–	–	1
MM5I_HadCM3	6	3	6	–	–	–	–	–
RCM3_CGCM3	2	–	9	2	–	–	1	1
RCM3_GFDL	2	–	10	2	–	–	1	–
WRFG_CCSM	4	1	8	2	–	–	–	–
WRFG_CGCM3	2	–	10	1	–	–	1	1
Future average	3.5	0.8	8.0	1.5	0.1	0.1	0.5	0.5
Change	+1.5	+0.8	+4.0	−4.5	−1.9	+0.1	−0.5	+0.5

compared with the baseline (Table 8). On average, the predicted snowfall decreased dramatically by 24% due a larger proportion of rainfall under warmer temperatures (Fig. 8b). Consequently, the total amount of snowmelt decreased significantly because of lesser snow accumulation. However, the spatial distribution of snowmelt showed that the frequency of snowmelt increased in late winter and earlier spring, though the peak of snowmelt decreased by more than 50%. The pattern of snowmelt suggested that instead of some major peaks of snowmelt in the baseline period, there would be more small peaks of snowmelt in the future (Fig. 9b).

The simulation results from future scenarios with only single factor changed showed that increased precipitation contributed to a greater amount of peak flows, increased snowfall and slightly decreased snowmelt. In contrast, increased temperature resulted in decreased amount of peak flows, decreased snowfall and a significant rise in snowmelt. The redistribution of peak flow events showed a rise in March and a decline in April. These were mainly the result of warming temperatures, because, in Quebec, the spring flow was dominated by snowmelt, while the summer and fall flows were attributed to the rainfall-runoff response (Troin and Caya, 2014).

When taking the factors of both precipitation and temperature into consideration, snowfall and snowmelt were projected to decrease by 6.5% and 4.4%, respectively. The increase in future temperature was the dominant factor affecting the total snowfall, which could offset the increased snowfall caused by increased precipitation. The pattern of snowmelt in the future was basically consistent with the snowmelt with only temperature changed. The increased volume of peak flow in the future was attributed to an increase in precipitation, while the advance of peak flow occurrence was a result of an increase in air temperature.

4. Conclusions

In this study, the ArcSWAT model was successfully parameterized

for the Nicolet River watershed. The model was calibrated using measured streamflow data from 1986 to 1990 and validated against similar data from 1991 to 2000. Statistical analysis suggested a satisfactory performance of the ArcSWAT model in simulating daily and monthly streamflow in both calibration and validation phases (NSE $>$ 0.5, RSR $<$ 0.7 and $|PBIAS| < 15\%$). Subsequently, eleven sets of projected future climate data were drawn upon by the calibrated and validated model, allowing future hydrologic responses to climate change in this study area to be simulated. Although annual precipitation was projected to increase in the future, the annual snowfall and the snowmelt would decrease by 6.5% and 4.4%, respectively due to warming temperatures. The snowmelt was projected to increase in late winter and early spring, though the snowmelt peaks would decrease by approximately 50%. An analysis of the individual impacts of temperature or precipitation implied that changes in the snowmelt pattern were attributed to the changing temperature. The reduction of snowfall decreased the snow stored in the snowpack, thus reducing the volume of snowmelt. The increased temperature induced more episodic snowmelt events and resulted in earlier snowmelt, such that the distribution of snowmelt events was altered.

The volume of annual peak flows was predicted to increase by 13% in the study region under climate change, suggesting a greater risk of future winter flooding events, with 11 peak flow events in the future on average compared with only 6 events in the baseline. Higher air temperatures in winter and spring would lead to earlier snowmelt, which consequently resulted in more frequent future peak flow events in the winter months, especially in March but less so in April, than under the baseline. Therefore, spring streamflow as well as associated peak flow events would decrease in the future, with the major peak flows in spring being more likely to be replaced by small peaks in the Nicolet River watershed. The current study provided an ArcSWAT modeling approach to estimate the future streamflow, timing and frequency of the peak flows as affected by snowmelt in Nicolet River watershed under climate change, which served a guideline for future water resource management and flood forecasting in the study region.

CRediT authorship contribution statement

Qianjing Jiang: Conceptualization, Writing - review & editing. **Zhiming Qi:** Conceptualization, Supervision, Writing - review & editing. **Fei Tang:** Visualization, Writing - original draft. **Lulin Xue:** Resources, Data curation. **Melissa Bukovsky:** Resources, Data curation.

Declaration of Competing Interest

The authors declare that they have no known competing financial interests or personal relationships that could have appeared to influence the work reported in this paper.

Acknowledgement

The research was funded by NSERC-Discovery Grant (Effect of management practices on hydrology and nutrient losses from a tile-drained field under freeze-thaw conditions), under Grant Agreement No. RGPIN-2019-05662.

Appendix A. Supplementary material

Supplementary data to this article can be found online at https://doi.org/10.1016/j.compag.2020.105756.

References

Arnell, N.W., Gosling, S.N., 2013. The impacts of climate change on river flow regimes at the global scale. J. Hydrol. 486, 351–364. https://doi.org/10.1016/j.jhydrol.2013.02.010.

Arnold, J.G., Moriasi, D.N., Gassman, P.W., Abbaspour, K.C., White, M.J., Srinivasan, R., Santhi, C., Harmel, R., Van Griensven, A., Van Liew, M.W., 2012a. SWAT: Model use, calibration, and validation. Trans. ASABE. 55, 1491–1508. https://doi.org/10.13031/2013.42256.

Arnold, J.G., Kiniry, J.R., Srinivasan, R., Williams, J.R., Haney, S., Neitsch, S.L., 2012b. Soil and Water Assessment Tool Input/Output Documentation, Version 2012, Texas Water Resources Institute, Temple, TX, USA. TR-439.

Arnold, J.G., Srinivasan, R., Muttiah, R.S., Williams, J.R., 1998. Large area hydrologic modeling and assessment part I: Model development1. J. Am. Water. Resour. AS. 34 (1). https://doi.org/10.1111/j.1752-1688.1998.tb05961.x.

Aygün, O., Kinnard, C., Campeau, S., 2019. Impacts of climate change on the hydrology of northern midlatitude cold regions. 0309133319878123. Prog. Phys. Geogr.: Earth Environ. https://doi.org/10.1177/0309133319878123.

Barnett, T.P., Adam, J.C., Lettenmaier, D.P., 2005. Potential impacts of a warming climate on water availability in snow-dominated regions. Nature 438, 303–309. https://doi.org/10.1038/nature04141.

Beauchamp, M., Assani, A.A., Landry, R., Massicotte, P., 2015. Temporal variability of the magnitude and timing of winter maximum daily flows in Southern Quebec (Canada). J. Hydrol. 529, 410–417. https://doi.org/10.1016/j.jhydrol.2015.07.053.

Bhatta, B., Shrestha, S., Shrestha, P.K., Talchabhadel, R., 2019. Evaluation and application of a SWAT model to assess the climate change impact on the hydrology of the Himalayan River Basin. Catena 181, 104082. https://doi.org/10.1016/j.catena.2019.104082.

Bhatta, B., Shrestha, S., Shrestha, P.K., Talchabhadel, R., 2020. Modelling the impact of past and future climate scenarios on streamflow in a highly mountainous watershed: A case study in the West Seti River Basin, Nepal. Sci. Total Environ. 140156. https://doi.org/10.1016/j.scitotenv.2020.140156.

Brooks, G., Evans, S., Clague, J., 2001. A synthesis of natural geological hazards in Canada. Geological Survey of Canada Bulletin. Natural Resources Canada. https://doi.org/10.4095/212210.

Burn, D.H., Elnur, M.A.H., 2002. Detection of hydrologic trend and variability. J. Hydrol. 255, 107–122. https://doi.org/10.1016/S0022-1694(01)00514-5.

CBC news, 2014. Quebec flood watch area growing. www.cbc.ca/amp/1.2600234.

Chen, J., Brissette, F.P., Leconte, R., 2011. Uncertainty of downscaling method in quantifying the impact of climate change on hydrology. J. Hydrol. 401, 190–202. https://doi.org/10.1016/j.jhydrol.2011.02.020.

Coulibaly, P., Anctil, F., Rasmussen, P., Bobee, B., 2000. A recurrent neural networks approach using indices of low-frequency climatic variability to forecast regional annual runoff. Hydrol. Process. 14, 2755–2777. https://doi.org/10.1002/1099-1085(20001030)14:153.3.CO;2-0.

Cunderlik, J.M., Ouarda, T.B.M.J., 2009. Trends in the timing and magnitude of floods in canada. J. Hydrol. 375 (3–4), 471–480. https://doi.org/10.1016/j.jhydrol.2009.06.050.

DesJarlais, C., Blondot, A., Allard, M., 2010. Learning to adapt to climate change. Ouranos.

ECCC. 2019. [Environment and Climate Change Canada] Canada's changing climate report. Available online at: https://changingclimate.ca/CCCR2019.

Ferguson, R., 1999. Snowmelt runoff models. *Prog. Phys. Geog.* 23, 205–227. https://doi.org/10.1177/030913339902300203.

Ficklin, D.L., Barnhart, B.L., 2014. SWAT hydrologic model parameter uncertainty and its implications for hydroclimatic projections in snowmelt-dependent watersheds. J. Hydrol. 519, 2081–2090. https://doi.org/10.1016/j.jhydrol.2014.09.082.

Gombault, C., Sottile, M.F., Ngwa, F.F., Madramootoo, C.A., Michaud, A.R., Beaudin, I., Chikhaoui, M., 2015. Modelling climate change impacts on the hydrology of an agricultural watershed in southern Québec. Can. Water Resour. J. 40, 71–86. https://doi.org/10.1080/07011784.2014.985509.

Grusson, Y., Sun, X., Gascoin, S., Sauvage, S., Raghavan, S., Anctil, F., Sáchez-Pérez, J., 2015. Assessing the capability of the SWAT model to simulate snow, snow melt and streamflow dynamics over an alpine watershed. J. Hydrol. 531, 574–588. https://doi.org/10.1016/j.jhydrol.2015.10.070.

Hammond, J.C., Saavedra, F.A., Kampf, S.K., 2018. How does snow persistence relate to annual streamflow in mountain watersheds of the Western US with wet maritime and dry continental climates? Water Resour. Res. 54 (4), 2605–2623. https://doi.org/10.1002/2017WR021899.

IPCC, 2013. Climate Change 2013: The Physical Science Basis. Contribution of Working Group I to the Fifth Assessment Report of the Intergovernmental Panel on Climate Change. Cambridge University Press, Cambridge, United Kingdom and New York, NY, USA.

Lachance-Cloutier, S., Turcotte, R., Cyr, J.F., 2017. Combining streamflow observations and hydrologic simulations for the retrospective estimation of daily streamflow for ungauged rivers in southern Quebec (Canada). J. Hydrol. 550, 294–306. https://doi.org/10.1016/j.jhydrol.2017.05.011.

Lemonds, P.J., McCray, J.E., 2007. Modeling hydrology in a small rocky mountain watershed serving large urban populations. J. AM. Water. Resour. AS. 43, 875–887. https://doi.org/10.1111/j.1752-1688.2007.00069.x.

Lévesque, E., Anctil, F., Van Griensven, A.N.N., Beauchamp, N., 2008. *Evaluation of streamflow simulation by SWAT model for two small watersheds under snowmelt and rainfall.* Hydrolog. Sci. J. 53 (5), 961–976. https://doi.org/10.1623/hysj.53.5.961.

Li, D., Wrzesien, M.L., Durand, M., Adam, J., Lettenmaier, D.P., 2017. How much runoff originates as snow in the western United States, and how will that change in the future? Geophys. Res. Lett. 44 (12), 6163–6172. https://doi.org/10.1002/2017GL073551.

López-Ballesteros, A., Senent-Aparicio, J., Martínez, C., Pérez-Sánchez, J., 2020. Assessment of future hydrologic alteration due to climate change in the Aracthos River basin (NW Greece). Sci. Total Environ. 139299. https://doi.org/10.1016/j.scitotenv.2020.139299.

Marin, M., Clinciu, I., Constantin, N., Cezar Ungurean, T., Adorjani, A., Mihalache, A.L., Davidescu, A.A., Davidescu, S.O., Dinca, L., Cacovean, H., 2020. Assessing the vulnerability of water resources in the context of climate changes in a small forested watershed using SWAT: A review. Environ. Res. 184, 0013–9351. https://doi.org/10.1016/j.envres.2020.109330.

Mearns, L.O., et al., 2007, updated 2014. The North American Regional Climate Change Assessment Program dataset, National Center for Atmospheric Research Earth System Grid data portal, Boulder, CO. Data downloaded 2016-07-24. https://doi.org/10.5065/D6RN35ST.

Mearns, L.O., Gutowski, W., Jones, R., Leung, R., McGinnis, S., Nunes, A., Qian, Y., 2009. A regional climate change assessment program for North America. EOS 90 (36), 311. https://doi.org/10.1029/2009EO360002.

Minville, M., Brissette, F., Leconte, R., 2008. Uncertainty of the impact of climate change on the hydrology of a nordic watershed. J. Hydrol. 358, 70–83. https://doi.org/10.1016/j.jhydrol.2008.05.033.

Moriasi, D.N., Arnold, J.G., Van Liew, M.W., Bingner, R.L., Harmel, R.D., Veith, T.L., 2007. Model evaluation guidelines for systematic quantification of accuracy in watershed simulations. Trans. ASABE. 50, 885–900. https://doi.org/10.13031/2013.23153.

Moriasi, D.N., Gitau, M.W., Pai, N., Daggupati, P., 2015. Hydrologic and water quality models: Performance measures and evaluation criteria. Trans. ASABE. 58, 1763–1785 10.13031/trans.58.10715.

Nash, J.E., Sutcliffe, J.V., 1970. River flow forecasting through conceptual models part I—A discussion of principles. J. Hydrol. 10 (3), 282–290. https://doi.org/10.1016/0022-1694(70)90255-6.

Neitsch, S.L., Arnold, J.G., Kiniry, J.R., Williams, J.R., 2011. Soil and water assessment tool theoretical documentation version 2009. Texas Water Resources Institute.

Noor, H., Vafakhah, M., Taheriyoun, M., Moghadasi, M., 2014. Hydrology modelling in Taleghan mountainous watershed using SWAT. J. Water Land Dev. 20, 11–18. https://doi.org/10.2478/jwld-2014-0003.

Rouhani, H., Leconte, R., 2018. A methodological framework to assess pmp and pmf in snow-dominated watersheds under changing climate conditions – a case study of three watersheds in Québec (Canada). J. Hydrol. 561, 796–809. https://doi.org/10.1016/j.jhydrol.2018.04.047.

Sharma, A., Wasko, C., 2019. Trends and Changes in Streamflow with Climate, in Trends and Changes in Hydroclimatic Variables, pp. 275–304. https://doi.org/10.1016/B978-0-12-810985-4.00005-0.

Shrestha, R.R., Dibike, Y.B., Prowse, T.D., 2012. Modelling of climate-induced hydrologic changes in the Lake Winnipeg watershed. J. Great Lakes Res. 38, 83–94. https://doi.org/10.1016/j.jglr.2011.02.004.

Shrestha, N.K., Du, X., Wang, J., 2017. Assessing climate change impacts on fresh water resources of the Athabasca River Basin. Canada. Sci. Total Environ. 601–602, 425–440. https://doi.org/10.1016/j.scitotenv.2017.05.013.

Singh, J., Knapp, H.V., Arnold, J., Demissie, M., 2005. Hydrological modeling of the iroquois river watershed using HSPF and SWAT1. J. AM. Water. Resour. AS. 41, 343–360. https://doi.org/10.1111/j.1752-1688.2005.tb03740.x.

St. Jacques, J.M., Sauchyn, D.J., 2009. Increasing winter baseflow and mean annual streamflow from possible permafrost thawing in the Northwest Territories, Canada. Geophys. Res. Lett. 36, L01401, 10.1029/2008GL035822.

Tang, G., Li, S., Yang, M., Xu, Z., Liu, Y., Gu, H., 2019. Streamflow response to snow regime shift associated with climate variability in four mountain watersheds in the US Great Basin. J. Hydrol. 573, 255–266. https://doi.org/10.1016/j.jhydrol.2019.03.021.

Troin, M., Caya, D., 2014. Evaluating the SWAT's snow hydrology over a Northern Quebec watershed. Hydrol. Process. 28, 1858–1873. https://doi.org/10.1002/hyp.9730.

Whitfield, P.H., Cannon, A.J., 2000. Recent variations in climate and hydrology in Canada. Can. Water Resour. J. 25, 19–65.

Wu, F., Zhan, J., Wang, Z., Zhang, Q., 2015. Streamflow variation due to glacier melting and climate change in upstream Heihe River Basin, Northwest China. Phys. Chem. Earth, Parts A/B/C 79, 11–19. https://doi.org/10.1016/j.pce.2014.08.002.

Wu, K., Johnston, C.A., 2007. Hydrologic response to climatic variability in a Great Lakes Watershed: A case study with the SWAT model. J. Hydrol. 337, 187–199. https://doi.org/10.1016/j.jhydrol.2007.01.030.

Yagouti, A., Boulet, G., Vincent, L., Vescovi, Luc, Mekis, É., 2008. Observed changes in daily temperature and precipitation indices for southern Québec, 1960–2005. Atmos. Ocean 46 (2), 243–256. https://doi.org/10.3137/ao.460204.

Yang, Y., Onishi, T., Hiramatsu, K., 2014. Improving the performance of temperature index snowmelt model of SWAT by using MODIS land surface temperature data. Sci. World J. 2014, 823424. https://doi.org/10.1155/2014/823424.

Zhang, L., Traore, S., Ge, J., Li, Y., Wang, S., Zhu, G., Cui, Y., Fipps, G., 2019. Using boosted tree regression and artificial neural networks to forecast upland rice yield under climate change in Sahel. Comput. Electron. Agr. 166, 105031. https://doi.org/10.1016/j.compag.2019.105031.

Zhang, X., Vincent, L.A., Hogg, W., Niitsoo, A., 2000. Temperature and precipitation trends in Canada during the 20th century. Atmos. Ocean 38, 395–429. https://doi.org/10.1080/07055900.2000.9649654.

Zhao, Q., Ding, Y., Wang, J., Gao, H., Zhang, S., Zhao, C., Xu, J., Han, H., Shangguan, D., 2019. Projecting climate change impacts on hydrological processes on the Tibetan Plateau with model calibration against the glacier inventory data and observed streamflow. J. Hydrol. 573, 60–81. https://doi.org/10.1016/j.jhydrol.2019.03.043.